Volume 4
Number 1
January 2026
Pages 1-454

RSC Applied Polymers

rsc.li/RSCApplPolym

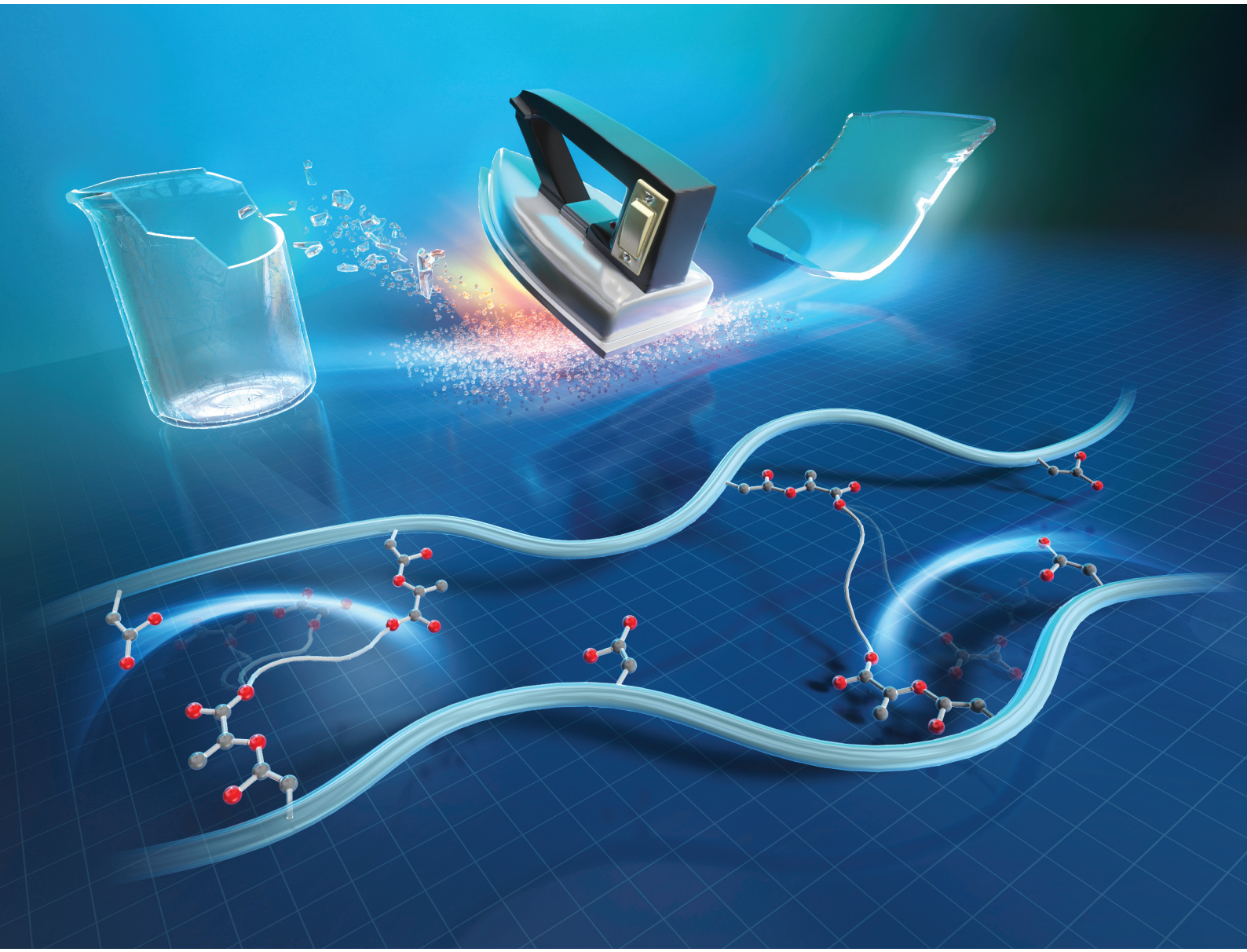

ISSN 2755-371X

ROYAL SOCIETY OF CHEMISTRY

PAPER
Yasuhiro Kohsaka, Mikihiro Hayashi *et al.*
Vitrimer-like acrylic glass with fast stress relaxation by high-speed carboxy exchange reaction

RSC Applied Polymers

ROYAL SOCIETY OF CHEMISTRY

PAPER

View Article Online
View Journal | View Issue

Cite this: *RSC Appl. Polym.*, 2026, **4**, 211

Vitrimer-like acrylic glass with fast stress relaxation by high-speed carboxy exchange reaction

Yasuhiro Kohsaka, *[a,b] Miu Mizuma[a] and Mikihiro Hayashi *[c]

We previously reported vitrimer-like acrylic elastomers in which the network structure was rearranged through high-speed carboxy exchange *via* the reversible conjugate substitution reaction of 2-(acyloxymethyl) acrylate. In this study, a similar chemistry was applied to vitrimer-like acrylic glass to investigate the effectiveness of the fast bond exchange reaction for a higher glass transition polymer with lower chain flexibility. The copolymer of methyl methacrylate and acrylic acid, derived from acid degradation of the *tert*-butyl acrylate unit, was cross-linked *via* a conjugate substitution reaction with 1,6-hexylene bis[(2-bromomethyl)acrylate]. Despite the high glass temperature, the obtained cross-linked acrylic glass doped with 1,4-diazabicyclo[2.2.2] octane (DABCO) exhibited fast stress relaxation with a relaxation time of 5.3 s at 140 °C. Fast stress relaxation led to excellent processability, affording a transparent, colorless film with a high modulus and tensile strength by hot-pressing within 2 min at 140 °C. A similar synthetic strategy was applied for the upcycling of a commercially available acrylic board, poly(methyl methacrylate). The hydrolysis and subsequent cross-linking reaction afforded a cross-linked polymer, which formed a transparent film after doping with DABCO. However, this film exhibited significantly slow stress relaxation, with a relaxation time of 136 s at 170 °C, probably because of the diffusion of polymer chains and DABCO restricted by long polymer chains.

Received 29th July 2025,
Accepted 21st October 2025

DOI: 10.1039/d5lp00241a

rsc.li/rscapplpolym

Introduction

Covalent adaptable networks (CANs), which are cross-linked polymers characterized by dynamic covalent bonds (DCBs), have attracted significant attention in the fields of polymer science and material engineering.[1–5] In stark contrast to traditional cross-linked polymers, CANs exhibit stress-relaxation behavior and enhanced processability owing to the facilitation of network structure rearrangement through bond-exchange reactions. Consequently, CANs are expected to be a novel class of polymer materials that combine recyclability and self-healing capabilities, attributed to their dynamic structure, with thermal stability, mechanical toughness, and chemical resistance, derived from their cross-linked architecture.

Vitrimers are a type of CANs characterized by bond-exchange reactions that occur through the formation of new bonds, followed by the dissociation of existing ones.[6–9] This 'associative' bond-exchange process allows the polymer network to rearrange without altering the cross-linking density, preventing a rapid decrease in viscosity as temperature rises. Typically, associative bond exchange is facilitated by addition–elimination or metathesis reactions, such as transesterification,[10–12] imine exchange,[13–15] and disulfide exchange.[16,17] Conversely, some bond-exchange reactions that follow an elimination–addition mechanism, such as quaternary ammonium exchange,[18,19] can also exhibit vitrimer-like behavior, provided that the dissociated intermediate has a sufficiently short lifetime, and rapid bond exchange is achieved. The dynamic properties of CANs, including vitrimers, stem from bond-exchange reactions and are thus under kinetic control. Consequently, fast bond-exchange reactions are essential for enhancing the performance of the vitrimers. This rapid bond exchange is achieved through substrates activated by neighboring groups[20,21] strong catalysts,[22] internal catalysts,[23,24] and rapid reactions.[25–27]

We recently reported vitrimer-like acrylic elastomers that exhibit remarkably rapid stress relaxation, driven by high-speed carboxy exchange.[28] This bond exchange relies on a reversible conjugate substitution reaction[29–32] between 2-(acyloxymethyl) acrylate and carboxylic acid, catalyzed by 1,4-diazabicyclo[2.2.2] octane (DABCO; Scheme 1A). Despite the dissociative mechanism, the intermediate was not detected in the model reaction using chloroform, a solvent with low polarity, suggesting a short lifetime for the intermediates. The intermediate is an ammonium carboxylate salt, in which ionic bonds facilitate

[a]*Faculty of Textile Science and Technology, Shinshu University, 3-15-1 Tokida, Ueda, Nagano 386-8567, Japan. E-mail: kohsaka@shinshu-u.ac.jp*
[b]*Research Initiative for Supra-Materials (RISM), Interdisciplinary Cluster for Cutting Edge Research (ICCER), Shinshu University, 4-17-1 Wakasato, Nagano, 380-8553, Japan*
[c]*Department of Life Science and Applied Chemistry, Graduate School of Engineering, Nagoya Institute of Technology, Gokiso-cho Showa-ku, Nagoya, Aichi, 466-8555, Japan. E-mail: hayashi.mikihiro@nitech.ac.jp*

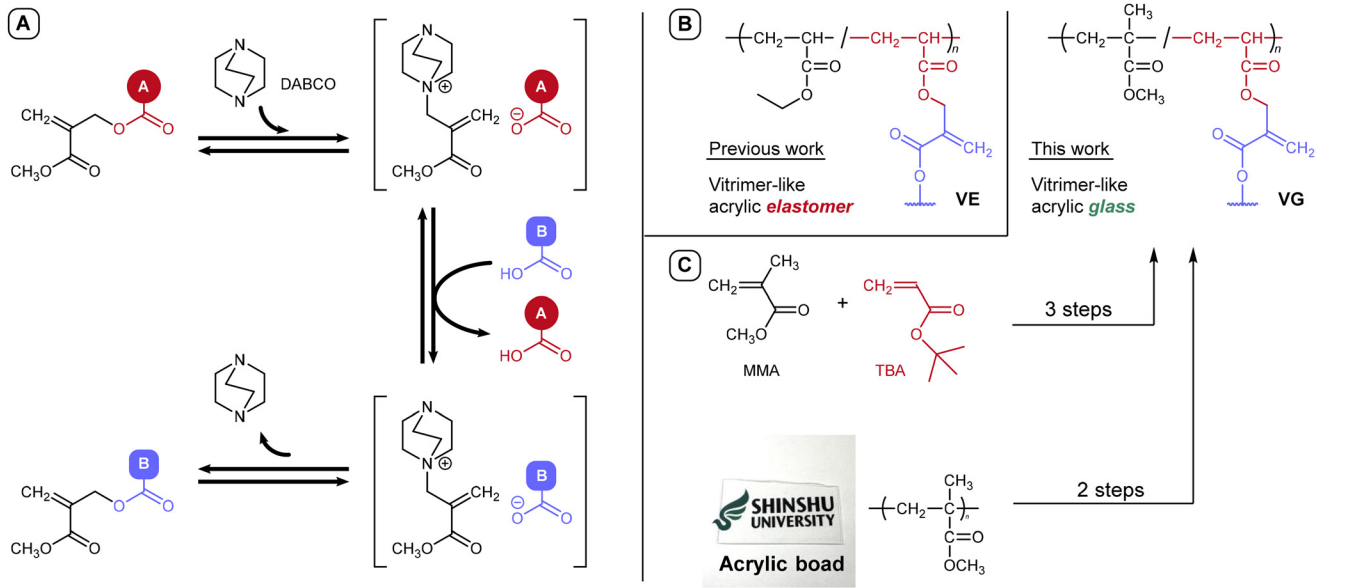

Scheme 1 Reversible bond exchange by high-speed carboxy exchange *via* conjugate substitution reaction (A). Vitrimer-like acryl polymers from previous (B) and current studies (C).

associative interactions. Consequently, the acrylic elastomers cross-linked through 2-(acyloxymethyl)acrylate frameworks (**VE**; Scheme 1B) functioned as vitrimer-like elastomers, offering rapid stress relaxation and excellent processability.

Rapid network rearrangement is necessary to achieve excellent dynamic characteristics in CANs and vitrimers, such as processability in a short time. This requires fast elementary reactions for bond exchange and sufficient diffusion of the reaction sites within the polymer network. Notably, vitrimers with higher glass transition temperatures (T_g), which are typically related to chain flexibility, generally exhibit slower stress relaxations. Thus, we were interested in the potential of high-speed carboxy exchange to provide superior vitrimer-like performance, even for high-T_g polymers such as acrylic glass (Scheme 1C). In addition to their vitrimer-like performance, transparent and colorless properties are also important for organic glasses. High-speed carboxy exchange does not require reactive sites or catalysts that cause coloration, which is also advantageous. Herein, we report a vitrimer-like organic glass with excellent processability and transparency prepared from copolymers of methyl methacrylate (MMA). Another of our interests is the upcycling of acrylic boards to vitrimer-like materials. Thus, we also report the application of our synthetic strategy to commercially available acrylic boards.

Experiments

Materials

Chloroform-d_1 ($CDCl_3$, 99.8 atom % D with 0.03 vol% tetramethylsilane) and dimethyl sulfoxide-d_6 (DMSO-d_6, 99.9 atom % D) were purchased from Kanto Chemical Co., Inc. DABCO, MMA, TBA were purchased from Tokyo Chemical Industry Co., Ltd. 2,2′-Azobisisobutyronitrile (AIBN), 1,4-dioxane, dichloromethane, *conc.* sulfuric acid, DMF and THF were purchased from Fujifilm Wako Pure Chemical Industry Co. 1,6-Hexylene bis[α-(bromomethyl)acrylate] (**3**) was purchased from Chemicrea Inc. Acrylic board was purchased from AS ONE Co.

Characterization of molecular structure

^{1}H NMR spectra were recorded in $CDCl_3$ or DMSO-d_6 using an AVANCE NEO spectrometer (Bruker). Chemical shifts in the ^{1}H NMR spectra were referenced to the signals of tetramethylsilane (TMS) and the solvent ($CHCl_3$ or DMSO). Molecular weight and its distributions were determined at 40 °C by size-exclusion chromatography (SEC) on an EXTREMA chromatograph (JASCO) equipped with two SEC columns [GPC HK-404L, Shodex], using chloroform (GPC grade, Fujifilm Wako Pure Chemical Industry) as an eluent (flow rate = 0.30 mL min^{-1}), and calibrated against standard poly(methyl methacrylate) (PMMA) samples (TSK-gel oligomer kit, Tosoh, M_n: 6.48×10^5, 2.52×10^5, 1.42×10^5, 2.91×10^4, 8.59×10^3, 4.25×10^3, 1.46×10^3, 8.30×10^2 g/mol) and detected with UV (UV-4070, 235 nm, JASCO) and RI (RI-4035, JASCO) detectors. IR spectra were recorded on a Cary 630 FTIR spectrometer equipped with a diamond-attenuated total reflection (ATR) accessory.

Dynamic mechanical analysis (DMA) and stress–relaxation test

Ai film with thickness of 0.25 mm was prepared by hot-pressing at 140 °C for 2 min. A disc-shaped sample with a diameter of 8 mm and approximately 0.25 mm thickness was measured. Temperature-sweep rheology was conducted using a shear-type rheometer, MCR102e (Anton Paar) and disposable 8 mm plate. The frequency was fixed at 1 Hz and a constant strain of 0.1% was applied. Cyclic cooling and heating measurements were performed at a rate of 5 °C min^{-1}.

Stress–relaxation tests for the cross-linked samples were conducted at various high temperatures using the same setup. The strain was fixed at 3%, which was within the linear regime. The samples for the measurements were initially dried under vacuum for 12 h, and all the above rheology measurements were conducted under N_2 gas to minimize the effects of moisture in air.

Tensile test

Tensile tests were performed on an AGS-500NX (Shimadzu) instrument using a dumbbell-shaped specimen with a thickness of 0.33 mm. The measurements were performed at 25 °C and an extension speed of 10 mm min^{-1}.

Synthesis of P1

A solution of MMA (2.00 g, 20.0 mmol), TBA (1.58 g, 11.7 mmol), and AIBN (82.5 mg, 0.502 mmol) in 1,4-dioxane (28.5 mL) was bubbled using nitrogen gas for 20 min, heated 70 °C for 2 h, and poured dropwise to a cosolvent of methanol/water (v/v = 1/1, 570 mL). The precipitate was collected by centrifugation, dissolved in THF, and dried *in vacuo* to afford 1.66 g (46.3%) of **P1**.

Synthesis of P2

P1 (1.65 g) was dissolved in dichloromethane (15 mL) and trifluoroacetic acid (2.49 g, 21.8 mmol) was added. The solution was stirred for 28 h and then poured dropwise into diethyl ether (300 mL). The precipitate was collected by centrifugation, dissolved in THF, and dried *in vacuo* to afford **P2** (1.15 g, 82.1%).

Preparation of P4 and VG

3 (0.313 g, 0.790 mmol) was added dropwise to a solution of **P2** (0.506 g) and triethylamine (0.160 g, 1.58 mmol) in THF (2 mL). The reaction mixture was allowed to stand for 3 h and then soaked in DMF (40 mL) for 12 h. The sol fraction was removed by decantation and the residual gel was soaked in DMF (40 mL) for 12 h. This procedure was repeated twice. A similar procedure was repeated thrice using THF instead of DMF. The residual gel was then dried *in vacuo* to obtain **P4** (0.508 g). **P4** swelled in a solution of DABCO (13 mg) in THF (2 mL) and dried *in vacuo* to afford **VG** (0.521 g).

Preparation of P6 and VG-R

P6 was prepared according to our recent report.[33] The obtained **P6** was converted to **VG-R** in a similar manner to the procedure on the conversion of **P4** to **VG**.

Results and discussion

Synthesis of vitrimer-like acrylic glass

In line with our previous research on acrylic elastomers,[28] we prepared vitrimer-like acrylic glass. The radical copolymerization of MMA (63 mol%) and *tert*-butyl acrylate (TBA; 37 mol%) was conducted in 1,4-dioxane using AIBN as the initiator (Scheme 2). The composition of the resulting copolymer, **P1**, was determined from the ^{1}H NMR spectrum (Fig. S1) to 71/29 for the MMA and TBA units. The *tert*-butyl ester pendants of the obtained copolymer **P1** were converted to carboxy groups using trifluoroacetic acid. The quantitative and selective pendant group conversion was confirmed by ^{1}H NMR (Fig. S2) and FTIR (Fig. S3) spectra. The obtained copolymer **P2** was treated with 1,6-hexylene bis[2-(bromomethyl)acrylate] (**3**) in the presence of triethylamine (TEA), ensuring that the bromine atoms of **3** were equimolar to the carboxy groups of **P2**. The resulting gel was swollen by immersing alternatively in *N*,*N*-dimethyl formamide (DMF) and THF, dried for 12 h three times to remove the byproduct of the bromide salt and sol fraction, and the residual gel was dried *in vacuo* to afford the cross-linked polymer **P4**. The weight fraction of the gel, that is, the yield of **P4**, was 74%.

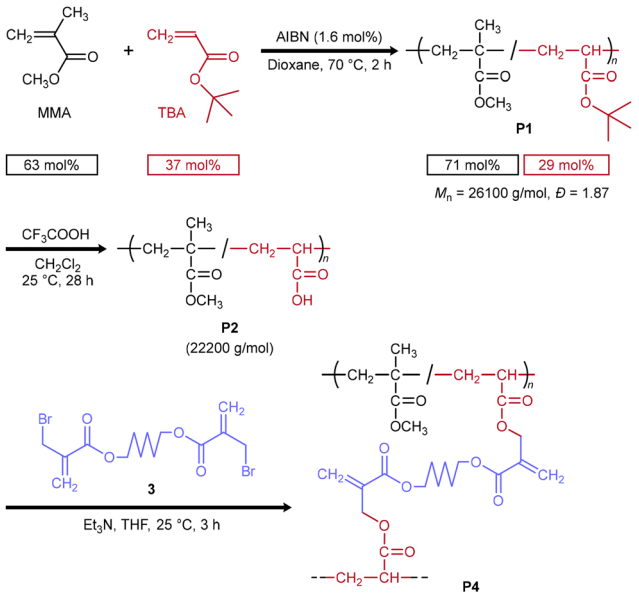

Scheme 2 Synthesis of cross-linked acrylic resin **P4**.

To enhance the bond exchange, the gel was swollen in a THF solution of DABCO and dried again *in vacuo*. The obtained resin (Fig. 1A) is denoted as **VG**. **VG** was hot pressed at 140 °C for 2 min under a pressure of 2 MPa, resulting in a colorless transparent film (Fig. 1B). The UV-vis spectrum of

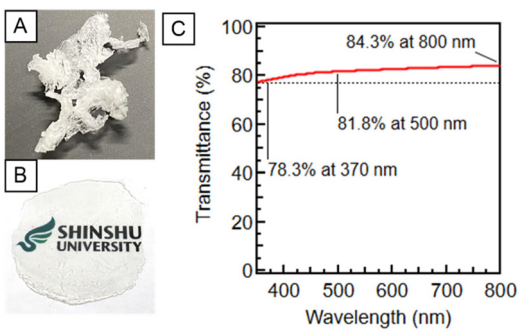

Fig. 1 **VG** before (A) and after (B) hot pressing, and the UV-vis spectrum of the obtained film with 0.15 mm thickness (C).

the film with 0.15 mm thickness (Fig. 1C) indicated 78–84% transmittance from 370 to 800 nm.

Thermal and mechanical properties

The dynamic mechanical analysis (DMA) of **VG** revealed a glass transition point (T_g) at 93 °C as the α-relaxation peak of tan δ (Fig. 2A). This indicates that **VG** was in the glass state at ambient temperature. The stress–strain curve of **VG** (Fig. 2B) presents typical characteristics of glass resins, such as a large modulus (1.29 GPa) and tensile strength (T_B; 35 MPa) with a small strain at break (E_B; 2.8%). In the DMA curve, the storage rubbery plateau modulus gradually decreased in a rubbery plateau region, especially above 150 °C. This is accompanied with the increase in the loss modulus (G'') and loss tangent (tan δ), which is related to fast stress relaxation comparable to the vibration frequency (1 Hz), was also observed for the vitrimer-like acryl elastomer **VE** in our previous report.[28]

The stress-relaxation curves of **VG** (Fig. S4) were normalized, as shown in Fig. 3A. The relaxation time (τ) was initially estimated according to the simple Maxwel model using the definition that the stress (σ) becomes 1/e of the initial value (σ_0). τ was 19 s and 5.3 s at 120 and 140 °C, respectively (Table 1). This relaxation rate is slightly slower but comparable to that of our previous low-T_g system (*i.e.*, **VE**), validating that the use of a carboxy exchange reaction *via* conjugate substitution into acryl glass-type materials could also be a powerful tool to achieve rapid stress relaxation. The temperature dependence of τ obeyed Arrhenius plots (Fig. 3B), suggesting that the network dynamics were governed by bond-exchange kinetics, which is known for vitrimers or other types of CANs.[34,35] To estimate the activation energy of the bond exchange (E_a) in the dynamic network, we adopted the most conventional protocol, simply deriving E_a from the slope of the Arrhenius plot in Fig. 3B. The E_a value was estimated to be 97 kJ mol^{-1}. This value is slightly larger than that of VE (Table 1). Note that other estimation protocols, such as those based on the temperature-dependence of shift factors or temperature-dependence of the peak top frequency of the loss modulus within the rubbery plateau when conducting the frequency sweep rheology,[36,37] would provide different values of E_a. Nevertheless, the values of E_a for **VE** and **VG** were derived from a common protocol, that is, the temperature dependence of τ. Therefore, the present comparison should have the meaning, indicating that the T_g or segmental dynamics would influence the bond exchange feature in the network, which is actually verified in another studies.[38]

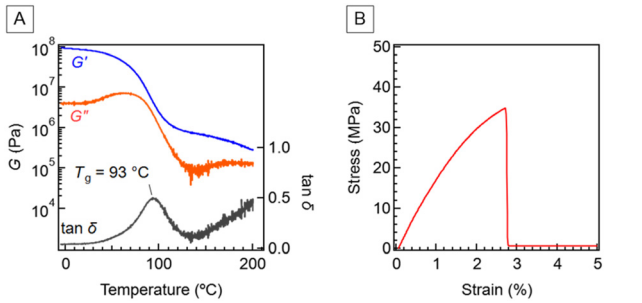

Fig. 2 Dynamic mechanical analysis (0.1% strain, 1 Hz, 5 °C min^{-1}) (A) and stress–strain curve (B, 10 mm min^{-1}) of **VG**.

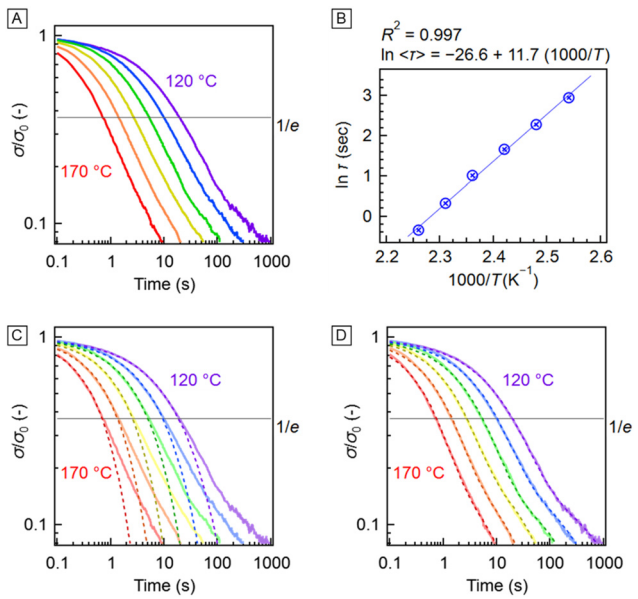

Fig. 3 Normalized stress-relaxation curves of **VG** (A) and their fitting analyses using eqn. (1) (C) and eqn. (2) (D). Arrhenius plots prepared from the stress-relaxation curves (B).

Table 1 Parameters for physical properties of **VE** and **VG**

#	T_g (°C)	E' (Pa)	T_B (MPa)	E_B (%)	τ (s) 140 °C	τ (s) 120 °C	E_a (kJ mol^{-1})
VE	19	2.4 M	1.8	65	2.5	7.0	74
VG	93	1.3 G	35	3	5.3	19	97

For fairer comparison of relaxation rate between **VE** and **VG** without considering the difference of T_g, we plotted the relaxation time as a function of the temperatures normalized by T_g of each sample, that is, (T–T_g); interestingly, **VG** exhibited shorter τ than **VE** (Fig. S5) in comparison with the normalized temperature. We assume that the relaxation rate, which should be dominated by the diffusion of the exchange unit in the network, is influenced by various molecular factors in the strand, such as the methyl substituent and length of the alkyl side group. In the future, we will clarify the essential factors that dominate the relaxation rate based on the versatile acylate or methacrylate sample series with different T_gs.

Curve-fitting analysis of the stress-relaxation curve was performed using Kohlrausch–Williams–Watts (KWW) functions (Fig. 3C), as shown in eqn (1).

$$\frac{\sigma}{\sigma_0} = \exp\left(-\frac{t}{\tau^*}\right)^{\beta} \quad (1)$$

where t, τ^*, and β are the time, specific relaxation time, and distribution of τ, respectively. However, apparent differences were observed between the fitted and experimental curves.

This result is similar to that of **VE**, which is in good agreement with the curves fitted according to eqn (2).[28]

$$\frac{\sigma}{\sigma_0} = A_f \exp\left(-\frac{t}{\tau_f}\right)^{\beta_f} + A_s \exp\left(-\frac{t}{\tau_s}\right)^{\beta_s} \quad (2)$$

This equation is based on the assumption of two relaxation modes, fast (f) and slow (s). This binary model is also effective for the curve-fitting analysis of the stress-relaxation curves of **VG** (Fig. 3D). Recently, Sain *et al.* introduced a combined model of dynamic and long-term relaxation modes.[39] The dynamic relaxation mode is driven by a bond exchange reaction and is fast, whereas the long-term relaxation mode is driven by diffusion and is slow. Chain entanglements, dispersity of cross-link density and molar mass, dangling chains, and other phenomena influencing molecular diffusion were hypothesized to explain the long-term relaxation. Since **P1**, the polymer precursor of **VG**, was prepared by free radical copolymerization, the molar mass and monomer sequence, that is, the location of the crosslinking point, should have a distribution. In addition, M_n was higher than the entanglement molar mass (M_e) of PMMA (*ca.* 10 000 g mol^{-1}).[40] Thus, a slow relaxation mode driven by diffusion effects was possible. However, except for our previous[28] and current reports, there are no examples of vitrimer-like materials that use the carboxy exchange reaction *via* conjugate substitution; thus, the reaction mechanism of bond exchange in a polymer matrix at high temperatures has not yet been deeply investigated. Consequently, a more detailed study and discussion are required to assign the origin of the slow relaxation mode.

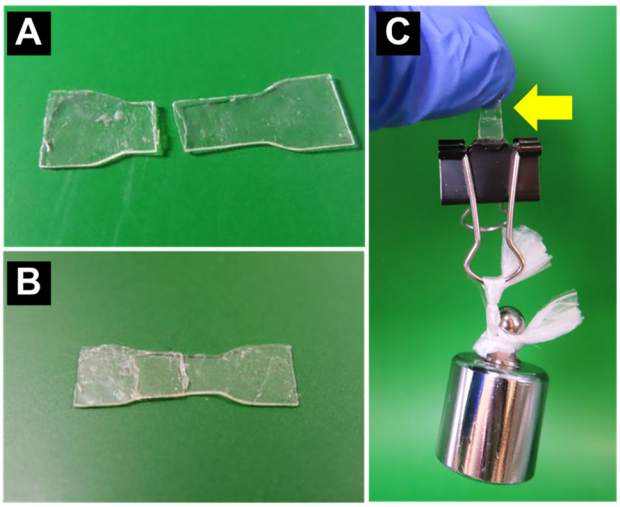

Fig. 4 Photographs of a cut film of **VG** (A) and the self-adhered film after heating with a houshold iron for 30s (B). The adhered film did not peel off even if a 100 g weight was hung (C). The yellow arrow indicates the adhered film.

Since the stress relaxation was so fast that 2 min was sufficient for hot pressing at 140 °C to produce a transparent film. Moreover, self-adhesion of the cut **VG** films was achieved by heating the films with household iron for 30 s (Fig. 4). Therefore, high-speed carboxy exchange is effective in imparting excellent processability even to cross-linked acrylic glass.

Upcycling of acrylic board

Finally, the upcycling of acrylic boards to vitrimer-like glass was investigated. Pristine PMMA is commercially available as acrylic boards, and we expected that the pendant modification of PMMA would provide vitrimer-like acrylic glass (Fig. 5A). Herein, an acrylic board prepared by a cell-casting method was used because it was composed of pure PMMA. The acrylic board was cut into small pieces (Fig. 5B) and mechanically crushed using a mixer mill (Fig. 5C). The resulting PMMA powder (**P3**) was dissolved in concentrated sulfuric acid, and the solution was heated at 50 °C for 10 min and poured into water.[32] The ^{1}H NMR spectrum of the resulting polymer, **P4**, suggested that the degree of hydrolysis was 10% (Fig. S6). **P4**

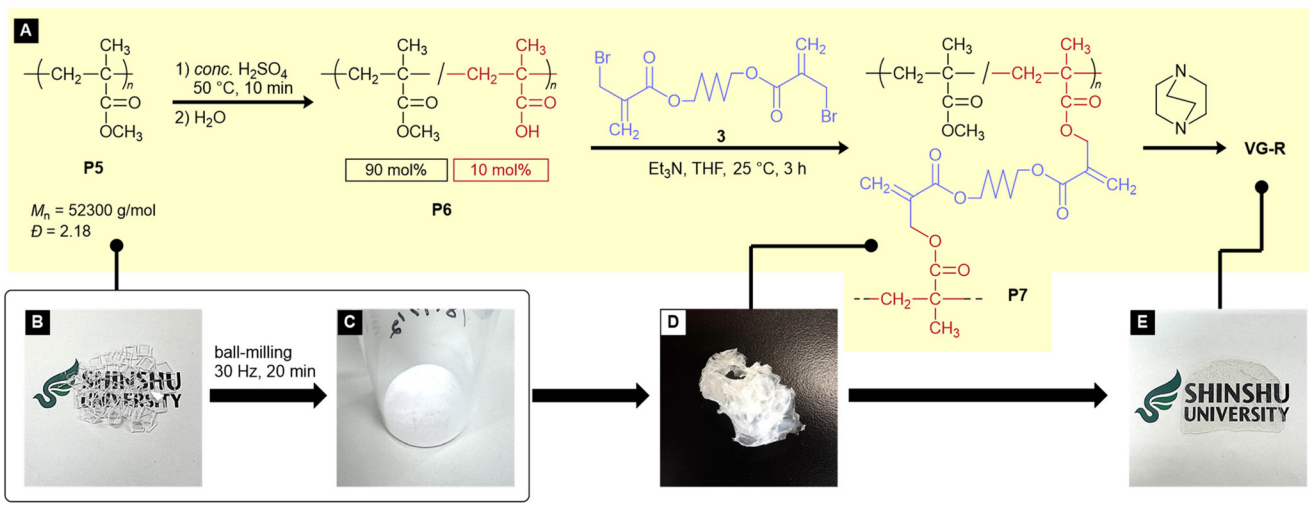

Fig. 5 Upcycling of an acrylic board to a vitrimer-like acrylic glass (A). Photographs in each step: the cut pieces (B) and crushed (C) of acrylic board. Cross-linked polymer (D) and its film prepared by hot-pressing after doping with DABCO (E).

was then cross-linked using **3** (Fig. 5D) and doped with DABCO in a manner similar to that of **P2** and **VG**. The obtained crosslinked polymer, coded **VG-R**, formed a transparent film by hot pressing at 100 °C for 2 min under 5 MPa pressure (Fig. 5E).

The DMA curves suggested the T_g of **VG-R** at 110 °C, which was higher than **VG** (Fig. S7). The G' value at 150 °C in the rubbery plateau region was 0.496 MPa, which was lower than that of **VG** (0.622 MPa). This tendency agreed with the composition of the mother polymers, **P2** and **P6**. Owing to the high T_g, the stress-relaxation test was conducted at temperatures of 150 °C and higher. Despite the excellent processability of **VG-R**, the stress relaxation was much slower than expected (Fig. S8 and S9). τ at 170 °C was 136 s, which was significantly longer than that of **VG** (0.71 s). Curve fitting using eqn (2) indicates that both τ_f and τ_s were much longer than those of **VG**, whereas the coefficients A_f and A_s were not significantly different (Table S2). The long τ_s implied restricted motion of the polymer chains. In fact, the SEC curves indicated that **P5**, the mother polymer of **VG-R**, had a fraction with molar masses higher than 900 000 g mol^{-1}, whereas **P1**, the mother polymer of **VG**, was composed of polymer chains with molar masses lower than 300 000 g mol^{-1} (Fig. S10). In general, a longer polymer chain causes larger entanglement effects and restricts diffusion. In addition, longer polymer chains have more cross-linking points, which also prevents diffusion. Such restricted diffusion is not limited to polymer chains but also affects the mobility of the catalyst and reactive groups. Indeed, the τ_f of **VG-R** was longer than that of **VG**, implying that the bond exchange reaction also decelerated. The Arrhenius plot (Fig. S11) indicated a higher activation energy of **VG-R** (160 kJ mol^{-1}) than **VG** (97 g mol^{-1}), which also implied the effects of diffusion on stress relaxation. However, more systematic experiments are desirable to discuss the effects of molar mass on diffusion and stress relaxation.

Conclusions

Acrylic glass cross-linked *via* 2-(acyloxymethyl)acrylate skeletons for high-speed carboxy exchange *via* a reversible conjugate substitution reaction exhibited processability in the presence of the DABCO catalyst, affording a transparent, colorless film with a large modulus and tensile strength. The film also exhibited fast stress relaxation owing to the high-speed carboxy exchange reaction. Thus, the carboxy exchange reaction was effective in imparting excellent dynamic properties to a wide range of polymers, from elastomers to glassy resins. Consequently, molecular strategies based on the conjugate substitution reaction are attractive for the design of vitrimer-like materials with transparency, mechanical toughness, processability, and excellent stress-relaxation performance. The preparation of vitrimer-like glass was also achieved by pendant modification (hydrolysis) and cross-linking of PMMA, commercially available as acrylic boards, although the stress relaxation was significantly slower than expected. This slow relaxation was anticipated to be related to the restricted diffusion of the polymer chains and catalysts, although more detailed experiments are required to reach a conclusion. This point will be reported in the future. The preparation of vitrimer-like glass was also achieved by pendant hydrolysis and cross-linking of PMMA, commercially available as acrylic boards, although the stress relaxation was significantly slower than expected. This slow relaxation was anticipated to be related to the restricted diffusion of the polymer chains and catalysts, although more detailed experiments are required to reach a conclusion. This point will be reported in the future.

Author contributions

YK: conceptualization, formal analysis, funding acquisition, visualization, methodology, project administration, resources, supervision, writing – draft. MM: data curation, formal analysis, investigation, validation, visualization, writing – review & editing. MH: funding acquisition, resources, supervision, writing – review & editing.

Conflicts of interest

Y. K. has a patent (Japanese Patent No. 7441526) on the cross-linking reaction and the cross-linked polymers issued to Shinshu University. The remaining authors declare no competing interests.

Data availability

The data supporting this manuscript is available as part of the supplementary information (SI). Supplementary information: ^{1}H NMR and IR spectra, SEC profiles, DMA curves, stress-relaxation curves, and their related plots. See DOI: https://doi.org/10.1039/d5lp00241a.

Acknowledgements

This research was financially supported by JST PRESTO Grant Numbers JPMJPR22N4 (for Y. K.) and JPMJPR23N7 (for M. H.).

References

1 G. M. Scheutz, J. J. Lessard, M. B. Sims and B. S. Sumerlin, *J. Am. Chem. Soc.*, 2019, **141**, 16181–16196.
2 C. J. Kloxin, T. F. Scott, B. J. Adzima and C. N. Bowman, *Macromolecules*, 2010, **43**, 2643–2653.
3 J. M. Winne, L. Leibler and F. E. Du Prez, *Polym. Chem.*, 2019, **10**, 6091–6108.
4 N. Zheng, Y. Xu, Q. Zhao and T. Xie, *Chem. Rev.*, 2021, **121**, 1716–1745.
5 M. Hayashi, *Polym. J.*, 2021, **53**, 779–788.

6 W. Denissen, J. M. Winne and F. E. Du Prez, *Chem. Sci.*, 2016, **7**, 30–38.
7 D. Montarnal, M. Capelot, F. Tournilhac and L. Leibler, *Science*, 2011, **334**, 965–968.
8 Q. Shi, C. Jin, Z. Chen, L. An and T. Wang, *Adv. Funct. Mater.*, 2023, **33**(16), 2300288.
9 M. Hayashi, *Polym. J.*, 2025, **57**, 343–355.
10 S. Debnath, S. Kaushal and U. Ojha, *ACS Appl. Polym. Mater.*, 2020, **2**, 1006–1013.
11 T. Isogai and M. Hayashi, *Macromol. Rapid Commun.*, 2024, **45**, e2400125.
12 T. Isogai and M. Hayashi, *Polym. Chem.*, 2024, **15**, 269–275.
13 K. Liang, G. Zhang, J. Zhao, L. Shi, J. Cheng and J. Zhang, *ACS Sustainable Chem. Eng.*, 2021, **9**, 5673–5683.
14 J. Liu, X. Liu, X. Cui, J. Qin, M. Shi, D. Wang, L. Liang and C. Yang, *ACS Appl. Polym. Mater.*, 2023, **5**(12), 10042–10052.
15 A. Vilanova-Pérez, S. De la Flor, X. Fernández-Francos, À. Serra and A. Roig, *ACS Appl. Polym. Mater.*, 2024, **6**, 3364–3372.
16 S. Guggari, F. Magliozzi, S. Malburet, A. Graillot, M. Destarac and M. Guerre, *Green Chem.*, 2025, **27**, 6392–6398.
17 S. Chai, Y. Fang, Z. Chen, D. Kong, S. Xiang, S. Zhao, F. Fu and X. Liu, *ACS Appl. Polym. Mater.*, 2025, **7**(6), 3981–3990.
18 A. Jourdain, R. Asbai, O. Anaya, M. M. Chehimi, E. Drockenmuller and D. Montarnal, *Macromolecules*, 2020, **53**, 1884–1900.
19 Y. Oba, T. Kimura, M. Hayashi and K. Yamamoto, *Macromolecules*, 2022, **55**, 1771–1782.
20 M. Delahaye, J. M. Winne and F. E. Du Prez, *J. Am. Chem. Soc.*, 2019, **141**, 15277–15287.
21 H. Zhang, S. Majumdar, R. A. T. M. van Benthem, R. P. Sijbesma and J. P. A. Heuts, *ACS Macro Lett.*, 2020, **9**, 272–277.
22 S. Bhusal, C. Oh, Y. Kang, V. Varshney, Y. Ren, D. Nepal, A. Roy and G. Kedziora, *J. Phys. Chem. B*, 2021, **125**, 2411–2424.
23 X. Feng and G. Li, *ACS Appl. Mater. Interfaces*, 2020, **12**, 57486–57496.
24 M. Hayashi, *ACS Appl. Polym. Mater.*, 2020, **2**, 5365–5370.
25 W. Denissen, G. Rivero, R. Nicolaÿ, L. Leibler, J. M. Winne and F. E. Du Prez, *Adv. Funct. Mater.*, 2015, **25**, 2451–2457.
26 J. J. Lessard, G. M. Scheutz, S. H. Sung, K. A. Lantz, T. H. Epps III and B. S. Sumerlin, *J. Am. Chem. Soc.*, 2020, **142**, 283–289.
27 Z. Wang, Y. Gu, M. Ma and M. Chen, *Macromolecules*, 2020, **53**, 956–964.
28 N. Nishiie, R. Kawatani, S. Tezuka, M. Mizuma, M. Hayashi and Y. Kohsaka, *Nat. Commun.*, 2024, **15**, 8657.
29 Y. Kohsaka, *Polym. J.*, 2020, **52**, 1175–1183.
30 Y. Kohsaka, Y. Akae, R. Kawatani and A. Kazama, *J. Macromol. Sci., Part A:Pure Appl. Chem.*, 2022, **59**, 83–97.
31 T. Noda, T. Kitagawa and Y. Kohsaka, *Polym. J.*, 2023, **56**, 343–351.
32 Y. Kohsaka, T. Yoshida and N. Nishiie, *Polym. Chem.*, 2025, **16**, 4009–4012.
33 Y. Chiba, S. Hirabayashi and Y. Kohsaka, *Chem. Sci.*, 2025, **16**, 12804–12811.
34 B. R. Elling and W. R. Dichtel, *ACS Cent. Sci.*, 2020, **6**, 1488–1496.
35 M. Hayashi and R. G. Ricarte, *Prog. Polym. Sci.*, 2025, **170**, 102026.
36 H. Fang, W. Ye, Y. Ding and H. H. Winter, *Macromolecules*, 2020, **53**, 4855–4862.
37 J. Luo, X. Zhao, H. Ju, X. Chen, S. Zhao, Z. Demchuk, B. Li, V. Bocharova, J.-M. Y. Carrillo, J. K. Keum, S. Xu, A. P. Sokolov, J. Chen and P.-F. Cao, *Angew. Chem., Int. Ed.*, 2023, **62**, e202310989.
38 S. Ge and C. M. Evans, *Macromolecules*, 2025, **58**, 4043–4058.
39 M. R. Karim, F. Vernerey and T. Sain, *Macromolecules*, 2025, **58**, 4899–4912.
40 S. Wu and R. Beckerbauer, *Polym. J.*, 1992, **24**, 1437–1442.